0νββ and 2νββ nuclear matrix elements, quasiparticle random-phase approximation, and isospin symmetry restoration

Fedor Šimkovic, Vadim Rodin, Amand Faessler, and Petr Vogel

$0\nu\beta\beta$ and $2\nu\beta\beta$ nuclear matrix elements, QRPA, and isospin symmetry restoration

Fedor Šimkovic*

*BLTP, JINR, 141980 Dubna, Moscow region, Russia and Comenius University, Mlynská dolina F1,
SK–842 48 Bratislava, Slovakia and IEAP CTU, 128–00 Prague, Czech Republic*

Vadim Rodin [†‡] and Amand Faessler[§]

Institute für Theoretische Physik der Universität Tübingen, D-72076 Tübingen, Germany

Petr Vogel[¶]

Kellogg Radiation Laboratory and Physics Department, Caltech, Pasadena, CA 91125, USA

Within QRPA we achieve partial restoration of the isospin symmetry and hence fulfillment of the requirement that the $2\nu\beta\beta$ Fermi matrix element $M_F^{2\nu}$ vanishes, as it should, unlike in the previous version of the method. This is accomplished by separating the renormalization parameter g_{pp} of the particle-particle proton-neutron interaction into the isovector and isoscalar parts. The isovector parameter $g_{pp}^{T=1}$ need to be chosen to be essentially equal to the pairing constant g_{pair}, so no new parameter is needed. For the $0\nu\beta\beta$ decay the Fermi matrix element $M_F^{0\nu}$ is substantially reduced, while the full matrix element $M^{0\nu}$ is reduced by $\approx 10\%$. We argue that this more consistent approach should be used from now on in the proton-neutron QRPA and in analogous methods.

I. INTRODUCTION

Answering the questions whether total lepton number is a conserved quantity or not, and thus whether neutrinos are massive Majorana fermions, is a crucial part of the search for the "Physics Beyond the Standard Model". Consequently, experimental searches for the $0\nu\beta\beta$ decay are pursued worldwide (for a recent review of the field, see e.g. [1]). However, interpreting existing results and planning new experiments is impossible without the knowledge of the corresponding nuclear matrix elements.

The nuclear matrix elements $M^{0\nu}$ of the $0\nu\beta\beta$ decay must be determined using nuclear structure theory, and the choice of the appropriate approximations is a crucial part of that task. Some of the methods employed for evaluation of the $M^{0\nu}$, in particular those that begin with the transformation from particles to quasiparticles to account for the like-nucleon pairing (see e.g. [2–8]), use wave functions that do not exactly conserve the particle number. The number of protons and neutrons is usually conserved on average or, in some cases, it is restored by the particle number projection. In either case, until now no attempt was made to check that the isospin, which is known to be, to a very good approximation, valid quantum number in nuclei, remains as such in the resulting wave functions that are obtained by solving the corresponding equations of motion.

It is well known that by the proper treatment of the quasiparticle interaction the broken symmetries can be restored. Naturally, exact calculation would restore the broken symmetries exactly. However, even with the approximate, RPA-like treatment, it is possible to partially restore some of the broken symmetries. In this work we show, following basically the suggestions made initially in Ref.[9], how this can be done in the case of isospin and by doing that the values of the Fermi nuclear matrix elements, both for the $2\nu\beta\beta$ and $0\nu\beta\beta$ decays, are substantially modified. Even though the resulting total $M^{0\nu}$ nuclear matrix elements are changed only by $\approx 10\%$, it is worthwhile, and certainly more consistent, to use in future the prescriptions described below.

II. FORMALISM

Assuming that the $0\nu\beta\beta$ decay is caused by the exchange of light Majorana neutrinos, the half-life and the nuclear matrix element are related through

$$\frac{1}{T_{1/2}^{0\nu}} = G^{0\nu}(Q,Z)|M^{0\nu}|^2 \, |\langle m_{\beta\beta}\rangle|^2 \, , \qquad (1)$$

where $G^{0\nu}(Q,Z)$ is the calculable phase space factor, $\langle m_{\beta\beta}\rangle$ is the effective neutrino Majorana mass whose determination is the ultimate goal of the experiments, and $M^{0\nu}$ is the nuclear matrix element consisting of Gamow-Teller, Fermi and Tensor parts,

$$M^{0\nu} = M_{GT}^{0\nu} - \frac{M_F^{0\nu}}{g_A^2} + M_T^{0\nu} \equiv M_{GT}^{0\nu}(1 - \chi_F/g_A^2 + \chi_T) \, , \qquad (2)$$

where χ_F and χ_T are the matrix element ratios $\chi_F = M_F^{0\nu}/M_{GT}^{0\nu}$ and $\chi_T = M_T^{0\nu}/M_{GT}^{0\nu}$. (In the literature a different notation is sometimes used, $\chi_F = M_F^{0\nu}/(g_A^2 M_{GT}^{0\nu})$.)

The main GT part, $M_{GT}^{0\nu}$, can be somewhat symbolically written as

$$M_{GT}^{0\nu} = \langle f|\Sigma_{lk}\sigma_l \cdot \sigma_k \tau_l^+ \tau_k^+ H(r_{lk}, \bar{E})|i\rangle \, , \qquad (3)$$

where $H(r_{lk}, \bar{E})$ is the neutrino potential described in detail in [5] and r_{lk} is the relative distance between the two neutrons that are transformed in the decay into the two protons.

Analogously, the Fermi matrix element is

$$M_F^{0\nu} = \langle f | \Sigma_{lk} \tau_l^+ \tau_k^+ H(r_{lk}, \bar{E}) | i \rangle . \tag{4}$$

Note that these $0\nu\beta\beta$ matrix elements are expressed in the closure approximation; its applicability is also discussed in [5]. However, the results reported later in this work were obtained without using the closure; instead explicit summation over all virtual intermediate states was performed.

The half-life of the experimentally well studied $2\nu\beta\beta$ decay depends formally on two nuclear matrix elements

$$\frac{1}{T_{1/2}^{2\nu}} = G^{2\nu}(Q, Z)[M_{GT}^{2\nu} + \frac{g_V^2}{g_A^2} M_F^{2\nu}]^2. \tag{5}$$

The Gamow-Teller $2\nu\beta\beta$ matrix element is

$$M_{GT}^{2\nu} = \Sigma_m \frac{\langle f || \Sigma_k \sigma_k \tau_k^+ || m \rangle \langle m || \Sigma_l \sigma_l \tau_l^+ || i \rangle}{E_m - (M_i + M_f)/2} , \tag{6}$$

where the summation extends over all 1^+ virtual intermediate states. In that case the closure approximation is not a valid approach but can be formally introduced by defining the corresponding closure matrix element $M_{cl}^{2\nu}$ when replacing the energies E_m by the proper average value $\bar{E}_{2\nu}$. Thus,

$$M_{GT(cl)}^{2\nu} \equiv \langle f | \Sigma_{lk} \sigma_l \cdot \sigma_k \tau_l^+ \tau_k^+ | i \rangle ,$$
$$M_{GT(cl)}^{2\nu} = M^{2\nu} \times (\bar{E}_{2\nu-GT} - (M_i + M_f)/2) . \tag{7}$$

Formally, in the description of the $2\nu\beta\beta$ decay also appears the Fermi matrix element

$$M_F^{2\nu} = \Sigma_m \frac{\langle f || \Sigma_k \tau_k^+ || m \rangle \langle m || \Sigma_l \tau_l^+ || i \rangle}{E_m - (M_i + M_f)/2} , \tag{8}$$

where the summation extends over all 0^+ virtual intermediate states, and its closure form is

$$M_{F(cl)}^{2\nu} \equiv \langle f | \Sigma_{lk} \tau_l^+ \tau_k^+ | i \rangle ,$$
$$M_{F(cl)}^{2\nu} = M_F^{2\nu} \times (\bar{E}_{2\nu-F} - (M_i + M_f)/2) . \tag{9}$$

The ground state $|i\rangle$ of the initial nucleus has isospin $T \equiv T_z = (N - Z)/2$ while the final state $|f\rangle$ has isospin $T - 2 \equiv T_z = (N - Z - 4)/2$. Since the operator $\Sigma_k \tau_k^+$ just changes the isospin projection and cannot change the total isospin, it is obvious that when isospin is a good quantum number both Fermi matrix elements must vanish,

$$M_F^{2\nu} = M_{F(cl)}^{2\nu} = 0, \tag{10}$$

since the average energy denominators in Eq. (9) are nonvanishing.

Until now, within QRPA, PHFB, EDF and IBM-2 methods the validity of condition Eq.(10) has not been usually tested ([2–8]). When results were published, $M_F^{2\nu}$ and $M_{F(cl)}^{2\nu}$ do not vanish and are, in fact, comparable to $M_{GT}^{2\nu}$ and $M_{GT(cl)}^{2\nu}$, respectively. Despite that, when evaluating the $2\nu\beta\beta$ half-life the Fermi matrix element was usually simply neglected.

As we show further, in the usual application of QRPA the condition Eq.(10) is not obeyed. Instead, the magnitude of $M_F^{2\nu}$ is numerically comparable to the magnitude of $M_{GT}^{2\nu}$ as just pointed out. In addition, for the $0\nu\beta\beta$ decay, within QRPA the ratio $\chi_F \approx -0.5$ while in the nuclear shell model, where isospin is a good quantum number by construction, the condition Eq.(10) is, naturally, obeyed and $\chi_F \approx -(0.2 - 0.3)$ [10].

Where does this problem in QRPA method originate? The method begins with the Bogoliubov transformation relating the particle creation and annihilation operators $a_{jm}^\dagger, \tilde{a}_{jm}$ with the quasiparticle creation and annihilation operators $c_{jm}^\dagger, \tilde{c}_{jm}$. By solving the BCS equations one includes the neutron-neutron and proton-proton isovector pairing interactions.

At this stage several symmetries are broken. The numbers of protons Z and neutrons N are no longer exact, but valid only on average. In addition, since the neutron-proton part of the isovector pairing interaction is neglected, additional source of isospin violation is introduced. It turns out that it is relatively easy to remedy this additional effect and restore the isospin conservation, at least in part, as explained further here. As the RPA (and QRPA) is derived from the equation of motion for bifermionic operators (treated in the quasiboson approximation), symmetries of the model Hamiltonian can naturally be fulfilled in that approximation.

To proceed further, the equations of motion need to be solved. Within the QRPA method the forward- and backward-going amplitudes X and Y that are needed for the evaluation of the nuclear matrix elements, as well as the corresponding energy eigenvalues ω_m, are determined by solving the eigenvalue equations of motion for each angular momentum and parity J^π

$$\begin{pmatrix} A & B \\ -B & -A \end{pmatrix} \begin{pmatrix} X \\ Y \end{pmatrix} = \omega \begin{pmatrix} X \\ Y \end{pmatrix} . \tag{11}$$

The matrices A and B are (see e.g. [11])

$$A_{pn,p'n'}^J = \tag{12}$$
$$\langle O | [(c_p c_n)^{(JM)\dagger}, [\hat{H}, (c_{p'}^\dagger c_{n'}^\dagger)^{(JM)}]] | O \rangle$$
$$= \delta_{pp'} \delta_{nn'} (E_p + E_n) -$$
$$(u_p v_n u_{p'} v_{n'} + v_p u_n v_{p'} u_{n'}) \times$$
$$2 g_{ph} \langle pn^{-1}, J | V | p'n'^{-1}, J \rangle$$
$$-(u_p u_n u_{p'} u_{n'} + v_p v_n v_{p'} v_{n'}) \times$$
$$2 g_{pp} \langle pn, J | V | p'n', J \rangle ,$$

and

$$B_{pn,p'n'}^J = \tag{13}$$

$$\langle O|[(c_p c_n)^{(J-M)}(-1)^M, [\hat{H}, (c_{p'} c_{n'})^{(JM)}]]|O\rangle$$
$$= -(u_p v_n v_{p'} u_{n'} + v_p u_n u_{p'} v_{n'})$$
$$\times 2g_{ph}\langle pn^{-1}, J|V|p'n'^{-1}, J\rangle$$
$$+(u_p u_n v_{p'} v_{n'} + v_p v_n u_{p'} u_{n'})$$
$$\times 2g_{pp}\langle pn, J|V|p'n', J\rangle ,$$

where E_p, E_n are the quasiparticle energies.

The definitions, Eqs. (12) and (13), contain two renormalization adjustable parameters g_{ph} for the particle-hole interaction, and g_{pp} for the particle-particle interaction. While $g_{ph} = 1.0$ is typically used, it is customary to adjust g_{pp} so that the experimentally known half-life of the $2\nu\beta\beta$ decay is correctly reproduced [2]. But the particle-particle neutron-proton interaction governed by g_{pp} actually contains two kinds of interaction matrix elements, isovector and isoscalar. Thus, to be consistent with the treatment of the like particle pairing, one should separate the $T = 1$ part from the $T = 0$ part, i.e. replace

$$g_{pp}\langle pn, J|V|p'n', J\rangle \rightarrow \qquad (14)$$
$$g_{pp}^{T=1}\langle pn, J, T = 1|V|p'n', J, T = 1\rangle$$
$$+g_{pp}^{T=0}\langle pn, J, T = 0|V|p'n', J, T = 0\rangle ,$$

and adjust the parameters $g_{pp}^{T=1}$ and $g_{pp}^{T=0}$ independently. To partially restore the isospin symmetry and achieve that Eq.(10) is obeyed, it is sufficient to choose $g_{pp}^{T=1} \sim g_{pair}$. (That the coupling constant of the isovector proton-neutron particle-particle force should be close, or identical, to the pairing strength constant, was recognized already in the early works on the QRPA application to the $\beta\beta$ decay that used a schematic, δ-force interaction, see Ref. [12]).

III. DETERMINATION OF THE PARAMETER $g_{pp}^{T=1}$

When solving the BCS pairing equations, it is customary to slightly renormalize the strength of the pairing part of the realistic nucleon-nucleon interaction so that experimental pairing gaps are correctly reproduced. Thus, four adjusted parameters $(d_{pp}^{(i)}, d_{pp}^{(f)}, d_{nn}^{(i)}, d_{nn}^{(f)})$ are introduced (see, e.g. [2–5]) representing the adjustments needed to describe the neutron and proton pairing gaps in the initial and final nuclei. The values of these parameters as well as their averages for selected $\beta\beta$-decay candidate nuclei are displayed in Table I. (The Table entries are for two variants of the nucleon-nucleon interaction and one choice, of large size (21/23 levels, oscillator shells $N = 0 - 5$ with the addition of the $i_{13/2}$ and $i_{11/2}$ for the nuclei heavier than ^{124}Sn), of the single particle level scheme. The results for other choices are not very different.) In several cases in Table I we encounter magic numbers of neutrons or protons. In those cases the BCS treatment is inappropriate and hence the corresponding entries are missing there. For the case of ^{48}Ca we considered two variants. In the listed one we assumed that there is no pairing in the doubly magic ^{48}Ca. In the other

variant we assumed that the values $\Delta_p = 2.18$ MeV and $\Delta_n = 1.68$ obtained from the usual odd-even mass difference with the five point formula represent the pairing gaps; the resulting $g_{pp}^{T=1}$ is rather similar to the values listed in Table I.
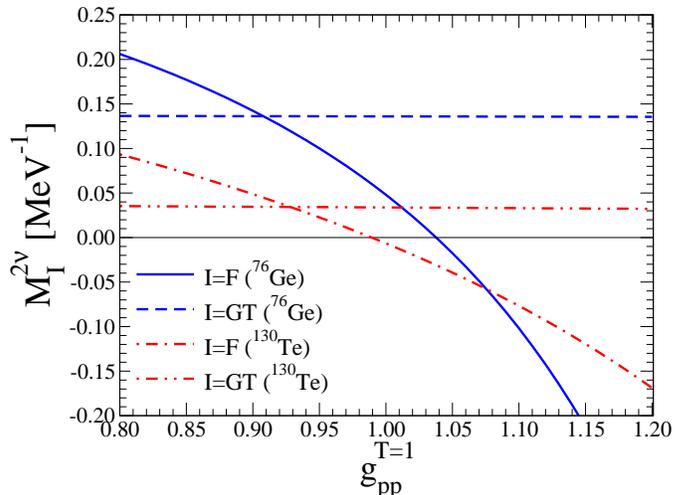
FIG. 1: (Color online) Dependence of the $2\nu\beta\beta$ matrix elements $M_F^{2\nu}$ and $M_{GT}^{2\nu}$ on the isovector coupling constant $g_{pp}^{T=1}$. This example is for ^{76}Ge and ^{130}Te, the Argonne V18 potential, and the isoscalar coupling constants $g_{pp}^{T=0} = 0.750$ and 0.783.

The example in Fig. 1 shows how the matrix elements $M_F^{2\nu}$ and $M_{GT}^{2\nu}$ behave when the isovector coupling constant $g_{pp}^{T=1}$ is changed while the isoscalar $g_{pp}^{T=0}$ is kept constant. As one can see, the Fermi matrix element $M_F^{2\nu}$ decreases and crosses zero, with increasing $g_{pp}^{T=1}$, while the Gamow-Teller matrix element remains constant. This is a typical case, and we can now choose $g_{pp}^{T=1}$ such that $M_{F-cl}^{2\nu}$ and hence also $M_F^{2\nu}$ vanish. Those values of $g_{pp}^{T=1}$ are shown in the last column of Table I.

It follows from the entries in Table I that the renormalization parameter $g_{pp}^{T=1}$ that assures the validity of the Eq. (10) is indeed very close to the average $\bar{d} \equiv g_{pair}$ of the pairing parameters $d_{ii}^{i,f}$. In few rare cases, in particular in semi-magic nuclei, the difference between $g_{pp}^{T=1}$ and $\bar{d}$ is $\sim 10\%$ (but not more). As shown in Ref. [9] the ratio $g_{pp}^{T=1}/\bar{d}$ remains essentially unchanged when the size of the single-particle basis is modified.

In this work, our choice is to renormalize $g_{pp}^{T=1}$ independently, but very close, to $\bar{d}$. On the other hand, it turns out that the $M_{GT}^{2\nu}$ depends sensitively only on $g_{pp}^{T=0}$, so that this parameter can be still adjusted such that the half-life of the $2\nu\beta\beta$ decay is correctly reproduced, exactly as done before. In fact, the previously used common value of g_{pp}, and the new parameter $g_{pp}^{T=0}$, are essentially the same as we demonstrate in the next Section.

TABLE I: Renormalization parameters of the pairing interaction, their average and the $T = 1$ renormalization constant $g_{pp}^{T=1}$ adjusted such that $M_{F(cl)}^{2\nu}$ and $M_F^{2\nu}$ vanish.

nucleus	NN pot.	number of s.p. lev	$d_{pp}^{(i)}$	$d_{nn}^{(i)}$	$d_{pp}^{(f)}$	$d_{nn}^{(f)}$	$\bar{d}$	$g_{pp}^{T=1}$
^{48}Ca	Argonne	21 lev.	—	—	1.075	0.988	1.034	1.031
	CD-Bonn	21 lev.	—	—	0.985	0.903	0.944	0.944
^{76}Ge	Argonne	21 lev.	0.930	1.074	0.970	1.106	1.020	1.038
	CD-Bonn	21 lev.	0.863	0.983	0.899	1.013	0.940	0.958
^{82}Se	Argonne	21 lev.	0.869	1.085	0.930	1.131	1.004	1.032
	CD-Bonn	21 lev.	0.808	0.995	0.864	1.038	0.926	0.955
^{96}Zr	Argonne	21 lev.	0.923	0.768	1.000	0.962	0.913	0.984
	CD-Bonn	21 lev.	0.856	0.704	0.926	0.881	0.842	0.907
^{100}Mo	Argonne	21 lev.	1.019	0.960	1.041	0.979	1.000	1.008
	CD-Bonn	21 lev.	0.946	0.883	0.966	0.900	0.924	0.933
^{110}Pd	Argonne	21 lev.	1.000	0.975	1.025	0.945	0.986	0.979
	CD-Bonn	21 lev.	0.930	0.895	0.954	0.871	0.913	0.908
^{116}Cd	Argonne	21 lev.	1.017	0.971	—	0.919	0.969	0.922
	CD-Bonn	21 lev.	0.949	0.895	—	0.847	0.897	0.852
^{124}Sn	Argonne	23 lev.	—	1.001	0.929	1.000	0.977	0.988
	CD-Bonn	23 lev.	—	0.918	0.860	0.917	0.898	0.913
^{128}Te	Argonne	23 lev.	0.881	0.968	0.926	0.999	0.944	0.988
	CD-Bonn	23 lev.	0.816	0.889	0.857	0.918	0.870	0.914
^{130}Te	Argonne	23 lev.	0.845	0.970	0.920	1.000	0.934	0.989
	CD-Bonn	23 lev.	0.783	0.891	0.852	0.918	0.861	0.915
^{134}Xe	Argonne	23 lev.	0.851	0.912	0.917	0.963	0.911	0.973
	CD-Bonn	23 lev.	0.790	0.840	0.850	0.887	0.842	0.903
^{136}Xe	Argonne	23 lev.	0.782	—	0.885	0.926	0.864	0.950
	CD-Bonn	23 lev.	0.726	—	0.821	0.853	0.800	0.881

IV. RESULTS AND DISCUSSION

In the previous Section we explained how the parameter $g_{pp}^{T=1}$ is determined. The determination of the other renormalization parameter $g_{pp}^{T=0}$ is analogous and follows the suggestion made long time ago in Ref. [2] as already stated. We fit $g_{pp}^{T=0}$ from the requirement that the calculated values of the full $2\nu\beta\beta$ matrix elements $M_{GT}^{2\nu}$ agrees with their experimental values. For most nuclei in Table I the half-lives $T_{1/2}^{2\nu}$ have been measured; we use the recommended values in Ref.[14] plus the ^{136}Xe half-life of Refs. [15, 16]. But for several nuclei in that Table, and in the Tables that follow, the half-life remains unknown. In those cases we proceed as follows: for ^{110}Pd we use the estimate of Ref. [17] that uses the single-state dominance assumption, for ^{124}Sn and ^{134}Xe we use an interval of possible $M_{GT}^{2\nu}$ values $0 \leq M_{GT}^{2\nu} \leq 0.2(0.1)\text{MeV}^{-1}$ for ^{124}Sn(^{134}Xe), respectively. For these two nuclei we show in Tables II - IV the results with $g_A = 1.0$ for the upper limit of $M_{GT}^{2\nu}$, and with $g_A = 1.27$ for the lower limit $M_{GT}^{2\nu} = 0$. Our results for these two nuclei therefore reflect our incomplete knowledge of the corresponding 2ν

half-life.

Before presenting the results for the $0\nu\beta\beta$ nuclear matrix elements, several comments are in order. Since the main effect considered here is the change in $M_F^{2\nu}$ and the associated change in $M_F^{0\nu}$, lets analyze these changes using the radial dependence of $M_{F-cl}^{2\nu}$ explained in Ref.[5]. In Fig. 2 the functions $C_{F-cl}^{2\nu}(r)$ with the old and new parametrization of g_{pp} are plotted, together with the function $C_{GT-cl}^{2\nu}(r)$ (scaled by 1/3 for clarity). As one can see, with the new $g_{pp}^{T=1}$ the tail of $C_{F-cl}^{2\nu}(r)$ becomes more negative and therefore its integral vanishes, as required. Let us remind ourselves that

$$M_{F-cl}^{2\nu} = \int_0^\infty C_{F-cl}^{2\nu}(r)dr , \qquad (15)$$

and in analogy

$$M_{GT-cl}^{2\nu} = \int_0^\infty C_{GT-cl}^{2\nu}(r)dr . \qquad (16)$$

Another comment concerns the fact that, as we will see, with the new parametrization $\chi_F \approx -(0.3 - 0.4)$, or more precisely $\chi_F \approx -1/3$. Somewhat similar conclusion
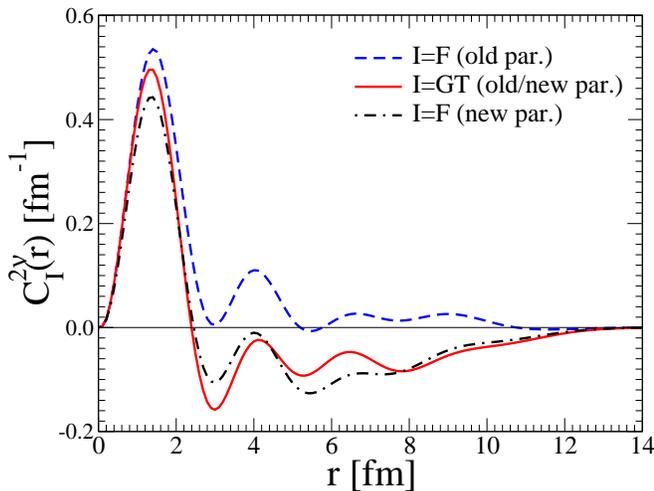
FIG. 2: (Color online) Functions $C_F^{2\nu}(r)$ with old and new parametrization and, for comparison, the function $C_{GT}^{2\nu}(r)$ (scaled by $1/3$ for clarity) is also shown. This is the case of ^{76}Ge.

is obtained in the shell model [10] where the isospin is conserved by definition. The explanation is based on the fact that the ground states of even-even nuclei consist dominantly of the $J^\pi = 0^+, T = 1$ Cooper pairs that, in turn, are mostly in the $S = 0, L = 0$ state. Since such states are eigenstates of the operator $\sigma_1 \cdot \sigma_2$ with eigenvalue -3, our conclusion simply follows.

In Fig. 3 we show examples of the decomposition of the function $C_{F-cl}^{2\nu}(r)$ into their $S = 0$ and $S = 1$ components. These are rather typical cases. The dominance of the $S = 0$ component in the pure pairing case (the upper panel in Fig. 3) is easily understood. However, that feature is still present in the realistic case with $g_{pp} \neq 0.0$, hence our finding that, usually, $\chi_F \approx -1/3$.

For both modes, $0\nu\beta\beta$ and $2\nu\beta\beta$, we can find relations between the Fermi and Gamow-Teller parts and their $S = 0$ and $S = 1$ components. These relations are exact in the closure approximation and when the higher order weak currents (and thus the tensor part $M_T^{0\nu}$) are neglected and the nucleon form factors have the same cut-off values for the vector and axial vector parts. In addition, since the neutrino potentials indirectly depend on the assumed averaged energy, these $\bar{E}$ values must be chosen to be the same for the Fermi and Gamow-Teller matrix elements. Using the properties of the $\sigma_1 \cdot \sigma_2$ operator and that $M_F^{2\nu} = 0$ with our new parametrization we find that only one of the four components is independent and

$$M_{cl-F}^{2\nu}(S = 0) = -M_{cl-F}^{2\nu}(S = 1) = \qquad (17)$$
$$= -M_{cl-GT}^{2\nu}(S = 1) = -M_{cl-GT}^{2\nu}(S = 0)/3 \; .$$

For the 0ν mode, however, $M_F^{0\nu} \neq 0$ and hence the above relations must be modified:

$$M_F^{0\nu}(S = 0) = M_F^{0\nu} - M_F^{0\nu}(S = 1) = \qquad (18)$$

$$= M_F^{0\nu} - M_{GT}^{0\nu}(S = 1) = -M_{GT}^{0\nu}(S = 0)/3 \; ,$$
$$M_{GT}^{0\nu} = M_F^{0\nu} - 4M_F^{0\nu}(S = 0) \; .$$

Two components are independent in this case. In realistic case these relations are not exact, but still valid in a reasonable approximation.

We will return to the discussion of the χ_F values obtained by different approximate methods in the next Section.
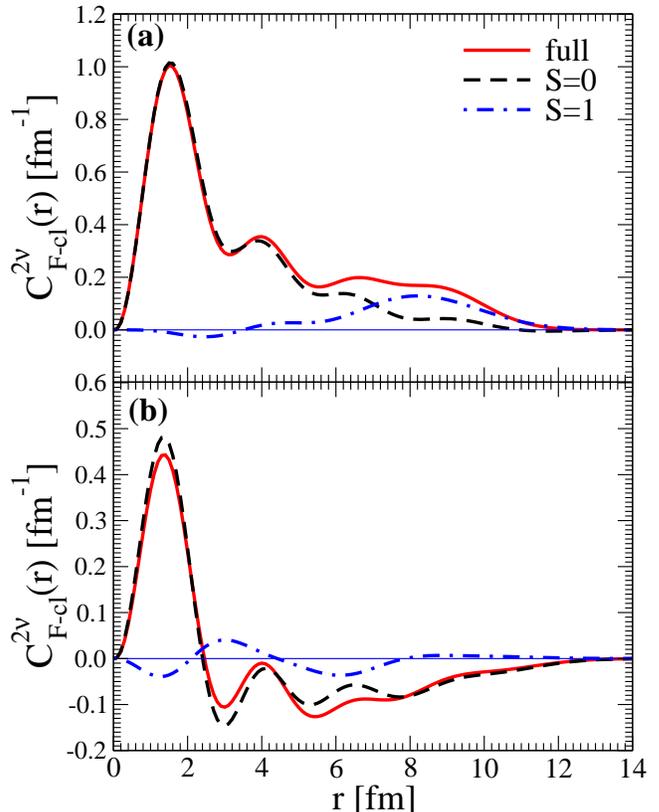
FIG. 3: (Color online) In the upper panel (a) the function $C_{F-cl}^{2\nu}(r)$ is shown for the pure pairing case, i.e. $g_{pp}^{T=0} = g_{pp}^{T=1} = g_{ph} = 0.0$, separated into the $S = 0$ and $S = 1$ components. In the lower panel (b) the function $C_{F-cl}^{2\nu}(r)$ is shown for $g_{pp}^{T=1} = 1.038$ and $g_{pp}^{T=0} = 0.750$ again separated into its $S = 0$ and $S = 1$ parts. The sum function is also displayed. The dominance of the $S = 0$ component is clearly visible in the upper panel. In the lower panel the two components when integrated over r are, naturally, equal and opposite. The $S = 0$ part, however, clearly is considerably larger in absolute value than the $S = 1$ part, at all r values. This is the case of ^{76}Ge.

In tables II and III we compare the resulting matrix elements $M_F^{2\nu}$, $M_{GT}^{2\nu}$ and $M^{0\nu}$ with its components evaluated using the old parametrization ($g_{pp}^{T=1} = g_{pp}^{T=0} \equiv g_{pp}$) with the new results, where $g_{pp}^{T=1} \approx g_{pair}$ and where $g_{pp}^{T=0}$

is fitted to the known experimental values of $M_{GT}^{2\nu}$. The calculations were performed for the unquenched value $g_A = 1.27$ as well as for $g_A = 1.0$. The quantities $M'^{0\nu} = M^{0\nu} \times (g_A/1.27)^2$ are also shown, as well as χ_F. Calculations in both tables were performed within the standard QRPA with all the usual ingredients, i.e. including the higher order weak currents, nucleon form factors, and the short-range correlation treatment of Ref. [13].

Lets explain briefly again (for more details see Ref. [5]) how the quenching is taken into account with our method. Since we adjust the isoscalar particle-particle renormalization constant $g_{pp}^{T=0}$ in such a way that the experimental half-life of the $2\nu\beta\beta$ is correctly reproduced, by changing the effective value of the axial current coupling constant g_A we are forced to change also the parameter $g_{pp}^{T=0}$, albeit only slightly. Those changes are visible in the third columns of Tables II and III. Since with smaller g_A the parameter $g_{pp}^{T=0}$ slightly decreases, the corresponding $M_{GT}^{0\nu}$ matrix element increases. However, the $0\nu\beta\beta$ decay rate, proportional to the $(M'^{0\nu})^2$, naturally, decreases.

In that context it is worthwhile to point out another feature of the new parametrization. The Fermi matrix element $M_F^{0\nu}$ is associated with the weak vector current, and as such should not be affected by the axial current quenching. With the old parametrization, with a single g_{pp}, that was not quite true, as seen in Tables II and III. However, with the new parametrization where isospin symmetry is partially restored, the $M_F^{0\nu}$ becomes independent of the effective value of g_A as it should be. (The tiny changes in Tables II and III are round-off errors.)

From the tables one can see that the new parametrization, leading to $M_F^{2\nu} = 0.0$, leads to a substantial reduction of the $M_F^{0\nu}$ component of $M^{0\nu}$ and overall $\sim$ 10-20% reduction of the final $M^{0\nu}$ nuclear matrix elements. It is encouraging that both variants of the $M^{0\nu}$ matrix elements for ^{48}Ca are now rather close to the results of nuclear shell model evaluation. (With $g_A = 1.27$ our $M^{0\nu}$ values are 0.54 in the listed case and 0.71 in the variant where the even-odd mass differences are treated as arising from pairing, both with the Argonne V18 potential and 0.59 (0.77) with the CD-Bonn potential , while the shell model values are 0.59 in Ref. [18] and 0.82(0.90) for the Argonne V18 (CD Bonn) potential in Ref.[19].) Note that only in the case of ^{48}Ca the full oscillator pf shell is included and hence the Ikeda sum rule is fulfilled in the nuclear shell model treatment. We are, naturally, well aware of the fact that to apply QRPA in the case of ^{48}Ca is questionable; our results should be treated with that in mind.

Finally, in order to better visualize effect of the new parametrization of the particle-particle interaction, we show in Fig. 4 an example of the multipole decomposition of the matrix element $M_F^{0\nu}$. One can see there that the contribution of the intermediate multipole 0^+ is drastically reduced with our choice of $g_{pp}^{T=1}$, while all the other multipoles are affected only slightly or not at all.

This is, in some sense, analogous to the situation with $M_{GT}^{0\nu}$ where the parameter $g_{pp}^{T=0}$ affects mostly the intermediate 1^+ states, while all the other multipolarities are affected much less.
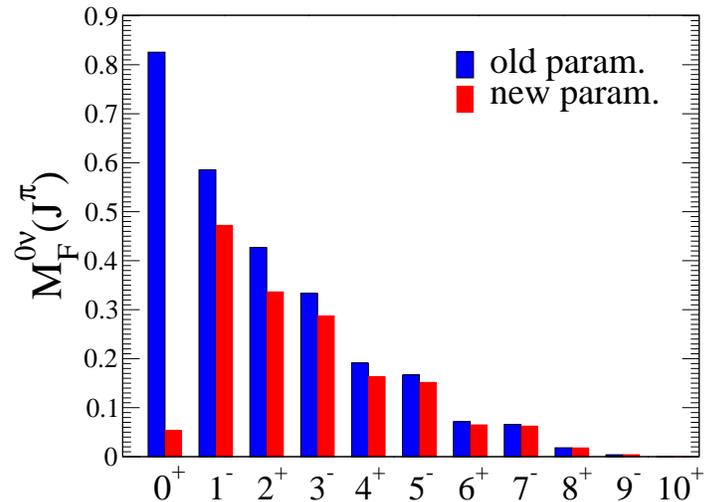
FIG. 4: (Color online) Multipole decomposition of the matrix element $M_F^{0\nu}$. The results with the old and new parametrizations are compared. Note the dominant effect for the 0^+ multipole, and the relatively small effects for the other multipoles. This is the case of ^{76}Ge.
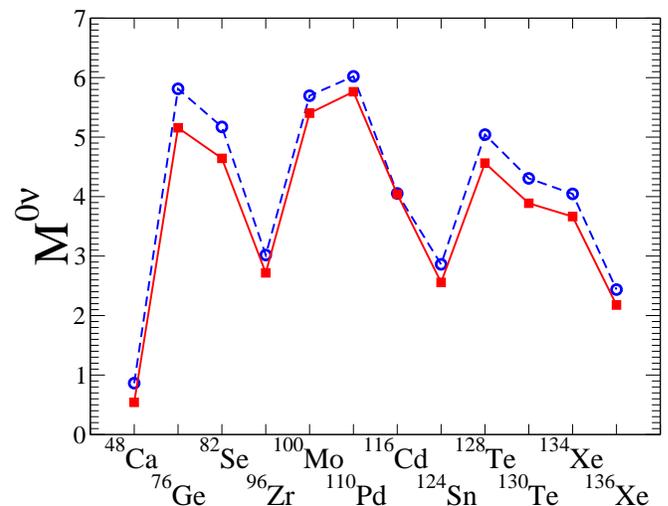
FIG. 5: (Color online) Nuclear matrix elements $M^{0\nu}$ evaluated with the new parametrization developed in this work (filled squares) compared with the old method ($g_{pp}^{T=1} = g_{pp}^{T=0} \equiv g_{pp}$) (empty circles). This is QRPA with $g_A = 1.27$ and large size single particle level scheme, as in Table I, evaluation using the Argonne V18 potential.

We compare in Fig. 5 the $M^{0\nu}$ matrix elements for all considered nuclei evaluated with the old and new parametrizations of g_{pp}. The smaller values of $M^{0\nu}$ in

^{48}Ca, ^{166}Cd, ^{124}Sn, ^{136}Xe and to some extent also in ^{96}Zr are related to the magic or semimagic nucleon number in these nuclei, and thus to the reduced pairing correlations in them.

V. COMPARISON OF THE χ_F VALUES EVALUATED BY DIFFERENT METHODS

As we argued in this work, the result of the new parametrization of the particle-particle interaction, that partially restores the isospin symmetry and leads to the correct $M_F^{2\nu} = 0$ value, is the reduction of the Fermi part $M_F^{0\nu}$ of the $0\nu\beta\beta$ nuclear matrix element. At the same time, the largest component of that matrix element, $M_{GT}^{0\nu}$, remains essentially unaffected. One can see that most clearly by considering the quantity χ_F, the ratio $M_F^{0\nu}/M_{GT}^{0\nu}$.

In Table IV we compare the χ_F values obtained with different methods. (Analogous table, naturally without our new results, appears in Ref. [20] in their Table VII. However, as we already mentioned, their definition of χ_F contains an extra factor $(g_V/g_A)^2$.) One can see in the Table IV that in the nuclear shell model, and in our QRPA calculation with the new parametrization of g_{pp}, the χ_F values are substantially smaller than in the previous approaches. (In IBM-2 the χ_F are very small when neutrons and protons are in different shells. That is an artifact of the model where only one shell in each system is included.)

In the shell model, and in our new QRPA calculations, the χ_F values are relatively close to -1/3, the value one would obtain in pure $S = 0$ states. However, in the shell model the χ_F values are systematically smaller than in our version of QRPA. Why this is so remains to be understood. (To be really precise, $\chi_F = -1/3$ would arise for pure $S = 0$ when the higher order terms in the weak current are absent, when in the nucleon form factor the cut-off parameters for the vector and axial vector currents are the same and the average energies $\bar{E}$ are the chosen to be the same in both neutrino potentials.) As we pointed out before, while the $S = 0$ component is large, the other parts, in particular $S = 1$, are clearly present.

We may notice that the QRPA values of χ_F are always smaller with the quenched value $g_A = 1.0$ compared to the unquenched value $g_A = 1.27$. That trend continues when the amount of quenching is increased, e.g. to $g_A = 0.8$ where χ_F values are really quite close to -1/3. However, the question of quenching of the $0\nu\beta\beta$ matrix elements remains open, and in particular how to treat it properly in the QRPA goes beyond the scope of the present paper.

VI. CONCLUSIONS

By separating the particle-particle neutron-proton interaction into its isovector and isoscalar parts, and renormalizing them each separately with its own fitted parameters $g_{pp}^{T=1}$ and $g_{pp}^{T=0}$, we have achieved the partial restoration of the isospin symmetry and fulfillment of the requirement that $M_F^{2\nu} = 0.0$. This has been done essentially without introducing new parameters, since $g_{pp}^{T=1} \approx g_{pair}$ as required by the isospin symmetry of the particle-particle force. At the same time the isoscalar parameter $g_{pp}^{T=0}$ is fitted from the requirement that the calculated $2\nu\beta\beta$ half-life is the same as its experimental value. The resulting $g_{pp}^{T=0}$ is then almost the same one as with the old parametrization with the single g_{pp} value.

When the new parametrization of the particle-particle renormalization constants is used in the QRPA evaluation of the $0\nu\beta\beta$ nuclear matrix elements, a substantial reduction of the Fermi part, $M_F^{0\nu}$, is observed, while the Gamow-Teller and Tensor parts remain essentially unaffected. The full matrix elements $M^{0\nu}$ are reduced by $\sim$ 10 -20% as seen in Fig. 5. We believe that such reduction, which also brings the ratio χ_F closer to $\approx -1/3$, nearer to its value in the isospin conserving nuclear shell model values, is realistic, and should be used in the future application of the QRPA and its generalizations.

[1] F. T. Avignone, S. R. Elliott and J. Engel, Rev. Mod. Phys. **8 0**, 481 (2008).

[2] V. A. Rodin, A. Faessler, F. Šimkovic and P. Vogel, Phys. Rev. C**68**, 044302(2003).

[3] V. A. Rodin, A. Faessler, F. Šimkovic and P. Vogel, Nucl. Phys. **A766**, 107 (2006), and erratum **A793**, 213 (2007).

[4] F. Šimkovic, A. Faessler, V. A. Rodin, P. Vogel, and J. Engel, Phys. Rev. C bf 77, 045503(2008).

[5] F. Šimkovic, R. Hodák, A. Faessler, and P. Vogel, Phys. Rev. C**83**, 015502(2011).

[6] T. R. Rodriguez and G. Martinez-Pinedo, Phys. Rev. Lett. **105**, 252503(2010).

[7] K. Chatuverdi, R. Chandra, P. K. Rath, P. K. Raina and J. G. Hirsch, Phys. Rev. C**78**, 054302 (2008).

[8] J. Barea and F. Iachello, Phys. Rev. C**79**, 044301 (2009).

[9] V. Rodin and A. Faessler, Phys. Rev. C**84**, 014322

(2011).

[10] E. Caurier, F. Nowacki, and A. Poves, Int. J. Mod. Phys. **E16**, 552 (2007); J. Menéndez, A. Poves, E. Caurier, and F. Nowacki, Nucl. Phys. A **818**, 139 (2009); E. Caurier, F. Nowacki and A. Poves; Eur. Phys. J.**A36**, 195 (2008).

[11] J. Suhonen, T. Taigel and A. Faessler, Nucl. Phys. **A486**, 91 (1988).

[12] P. Vogel and M. R. Zirnbauer, Phys. Rev. Lett. **57**, 3148 (1986); J. Engel, P. Vogel and M. R. Zirnbauer, Phys. Rev. C**37**, 731 (1988).

[13] F. Šimkovic, A. Faessler, H. Müther, V. Rodin, and M. Stauf, Phys. Rev. C**79**, 055501 (2009).

[14] A. S. Barabash, Phys. Rev. C**81**, 035501 (2010).

[15] N. Ackerman *et al.* , Phys. Rev. Lett. **107**, 212501 (2011).

[16] A. Gando *et al.* Phys. Rev.C**85**, 045504 (2012).

[17] D. Fink *et al.*, Phys. Rev. Lett. **108**, 062502 (2012).

[18] E. Caurier, J. Menendez, F. Nowacki and A. Poves, Phys. Rev. Lett. **100**, 052503 (2008).

[19] M. Horoi, arXiv: 1210.6680.

[20] J. Barea, J. Kotila, and F. Iachello, Phys. Rev. C**87**, 014315 (2013); arXiv:1301.4203 [nucl-th].

[21] J. Suhonen, private communications as quoted in [20].

[22] J. Suhonen, J. Phys. G**19**, 139 (1993).

TABLE II: Nuclear matrix elements for both $\beta\beta$ decay modes with the old parametrization ($g_{pp}^{T=0} = g_{pp}^{T=1} \equiv g_{pp}$) are compared to those with the new one, $g_{pp}^{T=0} \neq g_{pp}^{T=1}$. The adopted values of the parameter $g_{pp}^{T=0}$ are also shown. The results for two values of the axial coupling constant g_A are displayed; the quenched value $g_A = 1.0$ and the standard value $g_A = 1.27$. The G-matrix elements of realistic Argonne V18 potential nucleon-nucleon potential are considered. The nuclear radius $R = r_0 A^{1/3}$ with r_0 = 1.2fm is used.

nucleus	g_A	$g_{pp}^{T=0}$	param.	$M_F^{2\nu}$	$M_{GT}^{2\nu}$	$M_F^{0\nu}$	$M_{GT}^{0\nu}$	$M_T^{0\nu}$	$M^{0\nu}$	$M'^{0\nu}$	χ_F
^{48}Ca	1.000	0.771	old	0.331	0.0736	-0.794	0.642	-0.164	1.272	0.790	-1.24
		0.770	new	0.00	0.0736	-0.268	0.639	-0.161	0.745	0.463	-0.42
	1.27	0.776	old	0.327	0.0457	-0.788	0.526	-0.151	0.864	0.864	-1.50
		0.775	new	0.00	0.0457	-0.268	0.523	-0.149	0.541	0.541	-0.51
^{76}Ge	1.00	0.728	old	0.240	0.220	-2.688	5.276	-0.606	7.357	4.569	-0.51
		0.728	new	0.00	0.220	-1.612	5.236	-0.591	6.258	3.886	-0.31
	1.27	0.750	old	0.231	0.137	-2.632	4.753	-0.575	5.812	5.812	-0.55
		0.750	new	0.00	0.137	-1.615	4.715	-0.561	5.157	5.157	-0.34
^{82}Se	1.00	0.751	old	0.180	0.153	-2.394	4.614	-0.557	6.452	4.007	-0.52
		0.751	new	0.00	0.153	-1.529	4.586	-0.545	5.571	3.460	-0.33
	1.27	0.766	old	0.175	0.095	-2.359	4.233	-0.527	5.171	5.171	-0.56
		0.766	new	0.00	0.095	-1.531	4.207	-0.516	4.642	4.642	-0.36
^{96}Zr	1.00	0.806	old	0.063	0.145	-1.547	2.825	-0.414	3.958	2.458	-0.55
		0.817	new	0.00	0.145	-1.214	2.667	-0.411	3.469	2.154	-0.45
	1.27	0.824	old	0.058	0.090	-1.518	2.466	-0.391	3.018	3.018	-0.62
		0.830	new	0.00	0.090	-1.215	2.349	-0.387	2.717	2.717	-0.52
^{100}Mo	1.00	0.841	old	0.100	0.373	-2.757	5.166	-0.683	7.240	4.496	-0.53
		0.840	new	0.00	0.373	-2.250	5.162	-0.673	6.739	4.185	-0.44
	1.27	0.848	old	0.097	0.232	-2.738	4.640	-0.645	5.696	5.696	-0.59
		0.847	new	0.00	0.232	-2.251	4.639	-0.635	5.402	5.402	-0.49
^{110}Pd	1.00	0.785	old	0.081	0.423	-2.668	5.609	-0.585	7.692	4.777	-0.48
		0.783	new	0.00	0.423	-2.182	5.614	-0.574	7.222	4.485	-0.39
	1.27	0.805	old	0.075	0.263	-2.626	4.949	-0.558	6.021	6.021	-0.53
		0.803	new	0.00	0.263	-2.184	4.954	-0.549	5.762	5.762	-0.44
^{116}Cd	1.00	0.870	old	0.008	0.206	-1.633	3.663	-0.277	5.019	3.117	-0.45
		0.870	new	0.00	0.206	-1.583	3.661	-0.275	4.969	3.086	-0.43
	1.27	0.900	old	0.004	0.128	-1.607	3.319	-0.264	4.053	4.053	-0.48
		0.900	new	0.00	0.128	-1.586	3.318	-0.263	4.040	4.040	-0.48
^{124}Sn	1.00	0.628	old	0.132	0.20	-1.779	3.860	-0.344	5.295	3.288	-0.46
		0.626	new	0.00	0.20	-0.984	3.859	-0.338	4.504	2.797	-0.25
	1.27	0.785	old	0.086	0.00	-1.473	2.308	-0.361	2.861	2.861	-0.64
		0.785	new	0.00	0.00	-0.988	2.302	-0.358	2.558	2.558	-0.43
^{128}Te	1.00	0.770	old	0.133	0.0776	-2.540	4.453	-0.642	6.351	3.944	-0.57
		0.769	new	0.00	0.0776	-1.750	4.436	-0.634	5.552	3.445	-0.39
	1.27	0.780	old	0.128	0.0481	-2.508	4.092	-0.608	5.042	5.042	-0.61
		0.779	new	0.00	0.0481	-1.751	4.076	-0.601	4.563	4.563	-0.43
^{130}Te	1.00	0.775	old	0.103	0.0545	-2.232	3.796	-0.588	5.439	3.378	-0.59
		0.774	new	0.00	0.0545	-1.545	3.778	-0.582	4.742	2.945	-0.41
	1.27	0.784	old	0.100	0.0339	-2.206	3.493	-0.556	4.306	4.306	-0.63
		0.783	new	0.00	0.0339	-1.546	3.478	-0.550	3.888	3.888	-0.44
^{134}Xe	1.00	0.739	old	0.111	0.10	-2.247	4.108	-0.537	5.819	3.613	-0.55
		0.738	new	0.00	0.10	-1.501	4.091	-0.530	5.071	3.149	-0.37
	1.27	0.787	old	0.092	0.00	-2.112	3.256	-0.521	4.045	4.045	-0.65
		0.787	new	0.00	0.00	-1.513	3.241	-0.517	3.664	3.664	-0.47
^{136}Xe	1.00	0.730	old	0.0652	0.0313	-1.228	2.149	-0.299	3.078	1.911	-0.57
		0.730	new	0.00	0.0313	-0.806	2.138	-0.297	2.646	1.643	-0.38
	1.27	0.740	old	0.0627	0.0194	-1.211	1.968	-0.283	2.437	2.437	-0.62
		0.740	new	0.00	0.0194	-0.806	1.959	-0.282	2.177	2.177	-0.41

TABLE III: The same as in Table II for realistic charge-dependent Bonn potential (CD-Bonn).

nucleus	g_A	$g_{pp}^{T=0}$	param.	2νββ-decay NMEs		0νββ-decay NMEs					χ_F
				$M_F^{2\nu}$	$M_{GT}^{2\nu}$	$M_F^{0\nu}$	$M_{GT}^{0\nu}$	$M_T^{0\nu}$	$M^{0\nu}$	$M'^{0\nu}$	
^{48}Ca	1.000	0.703	old	0.321	0.0736	-0.795	0.678	-0.151	1.322	0.821	-1.17
		0.703	new	0.00	0.0736	-0.284	0.675	-0.149	0.810	0.503	-0.42
	1.27	0.708	old	0.318	0.0457	-0.789	0.558	-0.139	0.909	0.909	-1.41
		0.708	new	0.00	0.0457	-0.284	0.555	-0.137	0.594	0.594	-0.51
^{76}Ge	1.00	0.660	old	0.188	0.220	-2.794	5.644	-0.551	7.886	4.897	-0.49
		0.660	new	0.00	0.220	-1.711	5.607	-0.537	6.781	4.211	-0.30
	1.27	0.681	old	0.220	0.137	-2.735	5.052	-0.522	6.228	6.228	-0.54
		0.681	new	0.00	0.137	-1.713	5.018	-0.510	5.571	5.571	-0.34
^{82}Se	1.00	0.683	old	0.172	0.156	-2.495	4.939	-0.508	6.926	4.301	-0.51
		0.683	new	0.00	0.156	-1.616	4.913	-0.497	6.032	3.746	-0.33
	1.27	0.698	old	0.166	0.095	-2.459	4.508	-0.480	5.555	5.555	-0.55
		0.698	new	0.00	0.095	-1.618	4.484	-0.470	5.018	5.018	-0.36
^{96}Zr	1.00	0.735	old	0.060	0.145	-1.614	3.035	-0.373	4.276	2.655	-0.53
		0.747	new	0.00	0.145	-1.277	2.861	-0.370	3.769	2.341	-0.45
	1.27	0.753	old	0.055	0.090	-1.583	2.640	-0.351	3.271	3.271	-0.60
		0.760	new	0.00	0.090	-1.278	2.511	-0.347	2.957	2.957	-0.51
^{100}Mo	1.00	0.770	old	0.097	0.373	-2.883	5.532	-0.615	7.800	4.8435	-0.52
		0.769	new	0.00	0.373	-2.366	5.526	-0.606	7.287	4.525	-0.43
	1.27	0.778	old	0.093	0.232	-2.863	4.950	-0.580	6.148	6.148	-0.58
		0.776	new	0.00	0.232	-2.367	4.950	-0.571	5.850	5.850	-0.48
^{110}Pd	1.00	0.715	old	0.081	0.423	-2.799	6.046	-0.531	8.314	5.163	-0.46
		0.713	new	0.00	0.423	-2.288	6.052	-0.521	7.820	4.856	-0.38
	1.27	0.734	old	0.075	0.263	-2.755	5.324	-0.506	6.529	6.529	-0.52
		0.732	new	0.00	0.263	-2.290	5.330	-0.497	6.255	6.255	-0.43
^{116}Cd	1.00	0.785	old	0.010	0.206	-1.707	3.942	-0.253	5.396	3.351	-0.43
		0.784	new	0.00	0.206	-1.639	3.940	-0.251	5.328	3.308	-0.42
	1.27	0.815	old	0.006	0.128	-1.680	3.564	-0.241	4.367	4.367	-0.40
		0.814	new	0.00	0.128	-1.642	3.563	-0.240	4.343	4.343	-0.46
^{124}Sn	1.00	0.557	old	0.127	0.200	-1.871	4.208	-0.311	5.768	3.582	-0.44
		0.555	new	0.00	0.200	-1.057	4.206	-0.305	4.958	3.079	-0.25
	1.27	0.708	old	0.085	0.00	-1.569	2.579	-0.324	3.230	3.230	-0.61
		0.707	new	0.00	0.00	-1.062	2.575	-0.321	2.913	2.913	-0.41
^{128}Te	1.00	0.694	old	0.130	0.0776	-2.673	4.902	-0.580	6.996	4.344	-0.54
		0.693	new	0.00	0.0776	-1.850	4.887	-0.572	6.164	3.828	-0.38
	1.27	0.704	old	0.125	0.0481	-2.641	5.582	-0.549	5.582	5.582	-0.47
		0.703	new	0.00	0.0481	-1.851	4.476	-0.542	5.084	5.084	-0.41
^{130}Te	1.00	0.698	old	0.102	0.0545	-2.354	4.213	-0.531	6.036	3.748	-0.56
		0.697	new	0.00	0.0545	-1.637	4.198	-0.525	5.310	3.297	-0.39
	1.27	0.707	old	0.098	0.0339	-2.328	3.867	-0.502	4.810	4.810	-0.60
		0.706	new	0.00	0.0339	-1.637	3.852	-0.496	4.373	4.373	-0.42
^{134}Xe	1.00	0.664	old	0.110	0.10	-2.268	4.532	-0.486	6.414	3.983	-0.50
		0.663	new	0.00	0.10	-1.595	4.516	-0.479	5.632	3.497	-0.35
	1.27	0.712	old	0.092	0.00	-2.231	3.608	-0.472	4.522	4.522	-0.62
		0.712	new	0.00	0.00	-1.599	3.593	-0.466	4.119	4.119	-0.44
^{136}Xe	1.00	0.657	old	0.0643	0.0131	-1.300	2.395	-0.269	3.426	2.127	-0.54
		0.657	new	0.00	0.0313	-0.858	2.385	-0.268	2.975	1.847	-0.36
	1.27	0.667	old	0.0619	0.0194	-1.282	2.190	-0.255	2.735	2.735	-0.59
		0.667	new	0.00	0.0194	-0.858	2.181	-0.254	2.460	2.460	-0.39

TABLE IV: Ratio $\chi_F = M_F^{0\nu}/M_{GT}^{0\nu}$ (see our definition of χ_F in the Eq. (2)) in ISM [10], QRPA-A, QRPA-B (present work, $g_A = 1.00$ and $g_A = 1.27$ side by side), QRPA-A results are with the Argonne V18 potential, QRPA-B with the Bonn CD potential), IBM-2 [20], and QRPA-JyLa [21].

Nucleus			χ_F		
	ISM	QRPA-A	QRPA-B	IBM	QRPA-JyLa
^{48}Ca	-0.22	-0.42, -0.51	-0.42, -0.51	-0.68	-0.90^a
^{76}Ge	-0.16	-0.31, -0.34	-0.30, -0.34	-0.61	-0.35
^{82}Se	-0.16	-0.33, -0.36	-0.33, -0.36	-0.68	-0.45
^{96}Zr	—	-0.45, -0.52	-0.45, -0.51	-0.10	-0.69
^{100}Mo	—	-0.44, -0.49	-0.43, -0.48	-0.10	-0.64
^{110}Pd	-0.25	-0.39, -0.44	-0.38, -0.46	-0.05	-0.61
^{116}Cd	-0.30	-0.43, -0.48	-0.42, -0.46	-0.10	-0.45
^{124}Sn	-0.20	— -0.43	— -0.41	-0.56	-0.68
^{128}Te	-0.20	-0.39, -0.43	-0.38, -0.41	-0.55	-0.60
^{130}Te	-0.20	-0.41, -0.44	-0.39, -0.42	-0.55	-0.60
^{136}Xe	-0.20	-0.38, -0.41	-0.36, -0.39	-0.55	-0.60

[a] Ref.[22]